

Crystallization Behavior of Starch-Filled Polypropylene

Wanjun Liu, Ya-Jane Wang, Zhenhua Sun

Department of Food Science, University of Arkansas, 2650 N. Young Avenue, Fayetteville, Arkansas 72704

Received 20 March 2003; accepted 1 October 2003

ABSTRACT: Starches of different granule sizes, including corn, rice, and amaranth starches, were used to prepare starch-filled polypropylene (PP) and the effect of starch granule size on crystallization behavior of PP was investigated. Differential scanning calorimetry and scanning electron microscopy were used to monitor the energy changes of the crystallization of the melt and to characterize the morphology of PP/starch composites, respectively. Little interaction was observed between starch and PP despite the difference in starch granule size. The crystallization temperature of PP decreased with the addition of starch and this decrease became more apparent with increasing starch granule size. During nonisothermal crystallization, the dependency of the

relative degree of crystallinity on time was described by the Avrami equation. The addition of starch decreased the overall crystallization rate of PP, which was attributed to an increase in the activation energy of crystallization under nonisothermal conditions according to the Kissinger equation. An increase in starch granule size of starch would increase the crystallization activation energy of PP and consequently decrease its crystallization rate. © 2004 Wiley Periodicals, Inc. *J Appl Polym Sci* 92: 484–492, 2004

Key words: polypropylene (PP); starch; crystallization; melting; morphology

INTRODUCTION

Polypropylene (PP) is a thermoplastic and widely used in automobile, electrical equipment, furniture, and packaging industries because of its excellent and versatile properties. Many fillers were incorporated into PP matrix for cost reduction and it was later discovered that those fillers contributed functionality to the composites, such as improving the stiffness and mechanical properties and modifying the crystallization of the polymer.^{1–6} The structure and properties of the composites were affected by the source and structure of fillers and the interaction between the filler particles and polymeric matrix.^{1–4,6} Inorganic substances are the main filler materials used during the past decades. However, with an increased interest in biodegradable polymers, natural biopolymers, such as starch and cellulose, are being evaluated in the development of biodegradable products.^{6,7} Hamdan et al.⁸ reported that PP and sago starch were not compatible after noting that the tensile properties of the PP/sago starch blends decreased with increasing sago starch content even though sago starch granules were well

dispersed in the PP matrix.⁸ To improve the compatibility between PP and starch, Weil⁹ proposed using maleated PP instead of PP and the resultant PP/starch composites exhibited improved tensile strength. Li et al.¹⁰ and Bagheri¹¹ reported that starch had interactions with PP under processing conditions, thus inhibiting thermal degradation of PP and improving the flame-retardant properties of PP. However, few studies reported the effect of starch on the crystallization behavior of starch-filled PP.

This study was undertaken to understand the changes in crystallization behavior and morphology of PP/starch composites by differential scanning calorimetry (DSC) and scanning electron microscopy (SEM), respectively. The effect of starch granule size on crystallization of PP was also considered.

EXPERIMENTAL

Materials

Polypropylene, PP6219, with a melt flow rate (MFR) of 2.2 g/10 min and a density of 0.92 g/cm³, was purchased from Amoco Inc. (Houma, LA). Common corn starch was obtained from Cerestar USA, Inc. (Hammond, IN), native rice starch was a gift from A&B Ingredients Inc. (Fairfield, NJ), and amaranth starch was provided by Nu World Amaranth (Naperville, IL). Because of a high residual protein content, native rice and amaranth starches were further purified according to the method of Yang et al.¹²

Correspondence to: Y.-J. Wang (yjwang@uark.edu).
Contract grant sponsor: Agricultural Experiment Station, University of Arkansas.
Contract grant sponsor: Arkansas Rice Research and Promotion Board.

Preparation of composites

Blends of starch (corn, rice, or amaranth) and PP were premixed at room temperature using a KitchenAid mixer (St. Joseph, MI) with a weight fraction of 0.1. These mixtures were then melt-blended in a lab-scale twin-screw counterrotating extruder (PolyLab, ThermoHaake, Madison, WI) at 210°C and 50 rpm. The plain PP6219 was subjected to the same procedure, as were the blends.

Morphology observation

The blends were fractured in liquid nitrogen and the fracture surface was observed using a Hitachi S-2300 scanning electron microscope (Tokyo, Japan) at an accelerating voltage of 25 kV. The fracture surfaces were sputter coated with gold before examination.

Thermal analysis

The thermal properties of the blends were determined using a Perkin–Elmer Pyris-1 differential scanning calorimeter (DSC; Perkin Elmer Cetus Instruments, Norwalk, CT). Samples were heated from 50 to 220°C at a heating rate of 10°C/min, kept at 220°C for 10 min, then cooled to 50°C with different cooling rates of 40, 20, 10, or 5°C/min, and reheated to 220°C at a heating rate of 10°C/min. All operations were performed under a nitrogen purge and sample weights varied from 6 to 8 mg. The exothermic crystallization peak was recorded as a function of temperature. The relative degree of crystallinity X_t and the absolute degree of crystallinity X_c as a function of crystallization temperature T are defined, respectively, as

$$X_t = \int_{T_0}^T (dH_c/dT) dT / \int_{T_0}^{T_\infty} (dH_c/dT) dT \quad (1)$$

$$X_c = \int_{T_0}^T (dH_c/dT) dT / (1 - \phi)\Delta H_f^\circ \quad (2)$$

where T_0 and T_∞ represent the onset and end of crystallization temperature, respectively. $\Delta H = 159$ J/g is the heat of fusion for 100% crystalline PP and ϕ is the weight fraction of the filler in the blends.

RESULTS AND DISCUSSION

Morphology of PP and starch blends

The morphological structure of polymer blends is important because it ultimately determines many properties of the polymer blends, such as solid mechanical

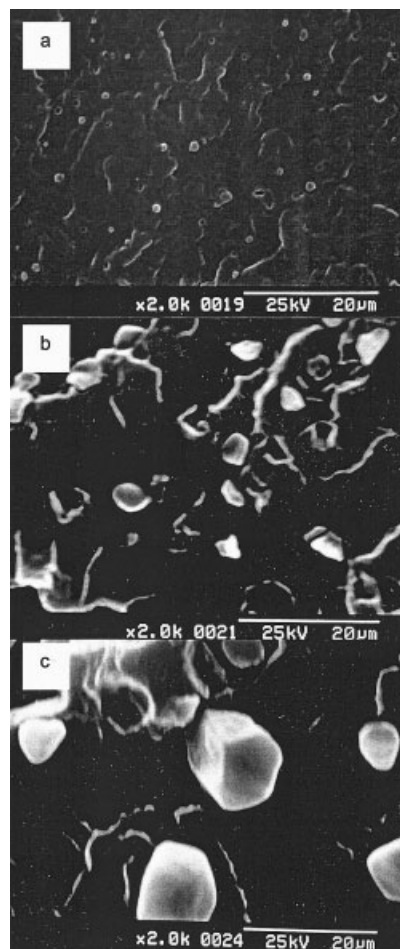


Figure 1 SEM micrographs of fracture surface of blends (a) PP/amaranth starch, (b) PP/rice starch, and (c) PP/corn starch.

and adhesive properties.¹³ Starch functioned as a filler in the PP/starch blends because the granular structure of starch was retained after extrusion and was homogeneously dispersed in the PP matrix as shown by SEM (Fig. 1). The miscibility of PP and starch was determined by the surface properties of starch and the structure of PP, given that starch was the filler. PP is known to be incompatible with starch because of the hydrophobic nature of PP and the hydrophilic nature of starch. However, it is not clear whether the starch granule size would change their interaction. The starch used in this study varied in average granule size, including amaranth starch of 1 μm , rice starch of 3 μm , and corn starch of 15 μm . The smooth surface and the distinct interfacial appearance of rice starch or corn starch and PP suggested that there was little interaction between them. In contrast, amaranth starch granules were surrounded by the PP matrix and the interface between them was less obvious, possibly from lower interfacial tension between amaranth starch and PP because of the small granule size of

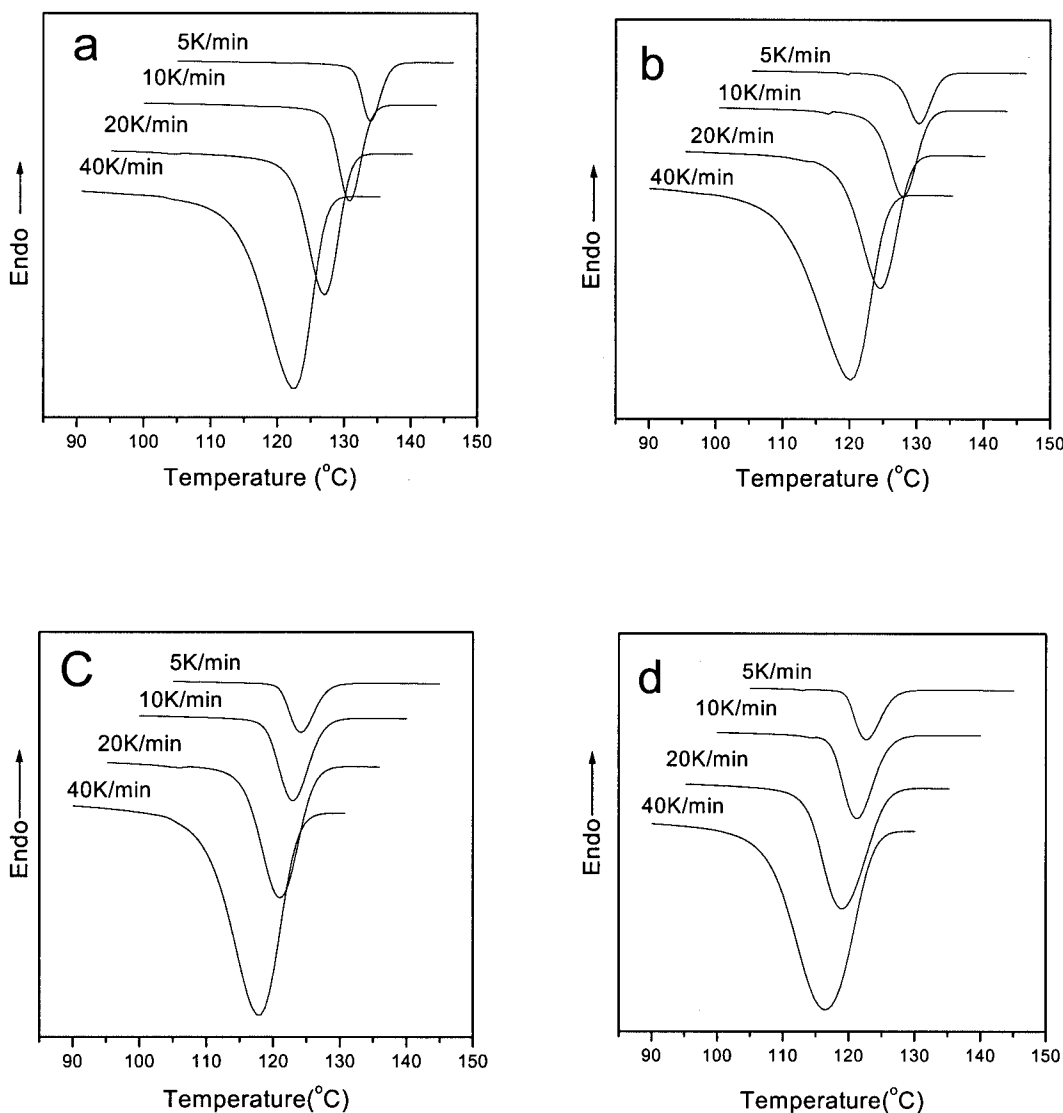


Figure 2 DSC curves during nonisothermal crystallization at different cooling rates of PP composites for (a) neat PP, (b) PP/amaranth starch, (c) PP/rice starch, and (d) PP/corn starch.

amaranth starch. The interfacial interaction between starch and PP is related to the granule size and surface property of starch. Although the surface property of starch from different sources is different, the granule size might be more important in contributing to their interaction because all starches were well dispersed in PP matrix. Therefore, the reason for possible different PP/starch interactions from different starches could be attributed to their differences in granule size, given that a decrease in particle size of the dispersed phase decreased the interfacial tension between the dispersed phase and the continuous phase.¹⁴

Crystallization behavior of PP and PP/starch composites

The DSC curves of PP and PP/starch composites at different cooling rates are depicted in Figure 2.

These DSC curves provided important parameters on the crystallization behavior of the composites, such as peak temperature denoted as crystallization temperature (T_c), corresponding peak time t_{max} , degree of crystallinity at T_c , crystallization enthalpy (ΔH) (Table I), and relative degree of crystallinity as a function of time (Fig. 3). The crystallization temperatures of PP and PP/starch composites shifted to lower temperatures with increasing cooling rates, presumably because polymer segments were not allowed a sufficient time to rearrange and crystallize. In this case, a higher supercooling was required to initiate crystallization. In addition, the segment motion of PP could not match the cooling temperature when the cooling rate was high. At a given cooling rate, crystallization temperatures of PP/starch composites were lower than that of PP, indi-

TABLE I
Effect of Starch on the Crystallization
Parameters of Polypropylene^a

| Sample | <i>P</i> (°C/min) | <i>T_c</i> (°C) | <i>t_{max}</i> (min) | <i>X_t</i> (%) | ΔH (J/g) |
|--------|----------------------|------------------------------|---------------------------------|-----------------------------|---------------------|
| PP | 40 | 122.2 | 0.20 | 37 | 89.58 |
| | 20 | 127.0 | 0.35 | 41 | 89.48 |
| | 10 | 130.9 | 0.63 | 43 | 91.55 |
| | 5 | 134.0 | 1.26 | 49 | 93.05 |
| PP-A | 40 | 120.2 | 0.27 | 34 | 80.26 |
| | 20 | 124.6 | 0.43 | 39 | 82.49 |
| | 10 | 128.0 | 0.71 | 42 | 83.69 |
| | 5 | 130.3 | 1.70 | 44 | 85.58 |
| PP-R | 40 | 118.2 | 0.33 | 37 | 76.04 |
| | 20 | 121.0 | 0.60 | 46 | 78.41 |
| | 10 | 122.9 | 1.45 | 52 | 78.39 |
| | 5 | 124.1 | 2.46 | 54 | 79.14 |
| PP-C | 40 | 116.8 | 0.30 | 41 | 75.66 |
| | 20 | 118.9 | 0.75 | 52 | 78.23 |
| | 10 | 121.2 | 1.66 | 53 | 78.78 |
| | 5 | 122.7 | 2.48 | 55 | 79.50 |

^a *P*, cooling rate during nonisothermal crystallization; *T_c*, crystallization temperature; *t_{max}*, time for maximum crystallization rate; *X_t*, relative degree of crystallinity at *T_c*; ΔH , crystallization enthalpy.

cating that starch did not have a nucleating effect but decreased the crystallization rate of PP. The negative impact on the crystallization of PP from starch can possibly be explained by two causes. One potential cause was that the addition of starch hindered the molecular motion of PP within the supercooling melt during cooling attributed to the interfacial tension of immiscible PP and starch.¹⁵ The other cause was that the presence of starch reduced the density of the nucleus and hindered the migration of PP to the nucleus.¹⁶ The negative influence from starch on the crystallization of PP became more pronounced with increasing starch granule size, demonstrating the difference between organic particles, such as starch, and inorganic particles, such as mica, CaCO₃, and rare earth oxides, which would promote the crystallization rate of PP blends.^{1,3-5}

Nonisothermal crystallization kinetics of PP and PP/starch composites

Crystallization kinetics of polymer is a complex phenomenon that encompasses several processes: production of primary nuclei, formation and spreading of bidimensional surface nuclei, and interdiffusion of crystallizable and noncrystallizable chains at the advancing front of the growing crystallites. These processes are affected to different

degrees by the thermodynamic conditions in which crystallization takes place, by the molecular structure characteristics, and by the interaction between polymer and filler. In general, the radial growth rate of the spherulites of polymer can be measured by means of polarized optic microscopy or DSC. The growth rate of the individual spherulity is usually measured by polarized optic microscopy, whereas the growth rate of the overall spherulites is conducted by DSC. According to the phenomenological theory, the relative degree of crystallinity achieved at time *t* is given by the Avrami equation^{17,18}

$$X_t = 1 - \exp(-kt^n) \quad (3)$$

where *n* is an index related to the dimensionality of growth and to the way primary nuclei are formed, and *k* is the overall rate constant including both nucleation and growth contribution. The Avrami equations can be rearranged in double-log form as

$$\log[-\ln(1 - X_t)] = \log k + n \log t \quad (4)$$

Linearization of eq. (2) enables one to evaluate *n* and *k* from the slope and the intercept, respectively, of the best straight lines fitting the experimental points at a low degree of transformation. The Avrami equation has been applied in analyzing isothermal crystallization of polymer.^{2,4} It also can be used to study crystallization under the nonisothermal condition; however, the values of *n* and *k* do not have the same physical significance as in the isothermal crystallization because the temperature changes constantly under nonisothermal condition. Therefore, *n* and *k* are two adjustable parameters to fit the data. Although the physical meaning of *n* and *k* could not be related in a simple way to the nonisothermal condition, the Avrami equation still provided insight into the kinetics of nonisothermal crystallization. The plots of $\log[-\ln(1 - X_t)]$ versus $\log t$ are displayed in Figure 4 and the crystallization parameters, such as Avrami index *n* and crystallization rate constant *k*, are listed in Table II.

The effect of starch granule on crystallization of PP was evident from Table II that the addition of starch decreased the rate of crystalline phase formation. The apparent overall rate constant as a function of temperature is listed for various PP/starch blends. The crystallization rate was characterized by half crystallization time *t*_{1/2}, which was obtained from Figure 3 and the incorporation of starch reduced the crystallization rate of PP, as demonstrated by the increased *t*_{1/2} of PP. At a given cooling rate, the crystallization rate of

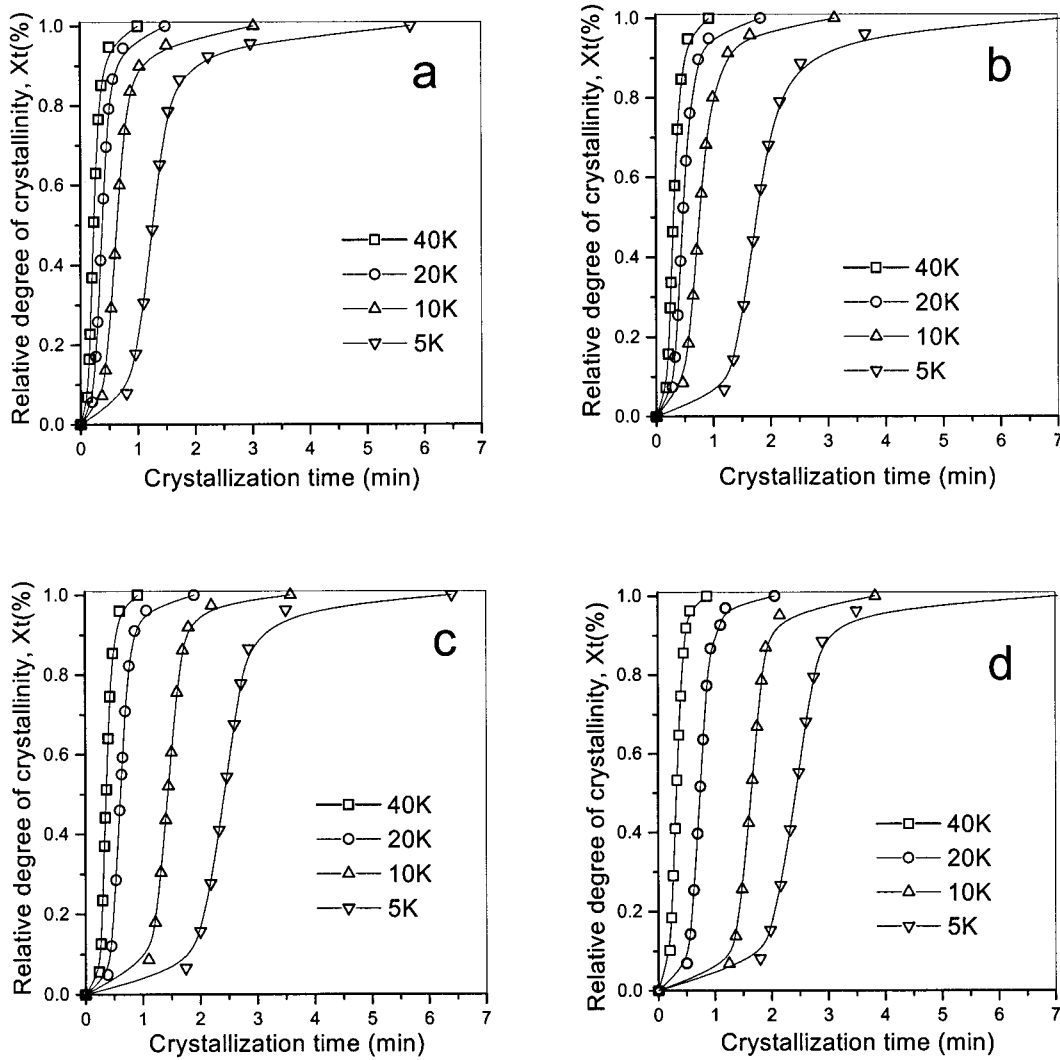


Figure 3 Relative crystallinity versus crystallization time during nonisothermal crystallization at different cooling rates of PP composites for (a) neat PP, (b) PP/amaranth starch, (c) PP/rice starch, and (d) PP/corn starch.

PP/starch composites followed the order of PP/amaranth starch > PP/rice starch > PP/corn starch, indicating that starch granule size was an important parameter affecting its crystallization behavior of PP/starch composites. The addition of amaranth starch had little effect on the absolute degree of crystallinity of PP; however, the addition of corn starch or rice starch decreased the absolute degree of crystallinity of PP. These results suggested that amaranth starch affected only the crystallization rate of PP crystal but rice starch or corn starch affected both the quantity and the rate of crystal growth of PP.

Ozawa¹⁹ modified the Avrami equation to account for the effect of cooling rate on dynamic crystallization. According to Ozawa's theory, the degree of conversion at temperature T , X_t , was expressed as

$$1 - X_t = \exp[-K(T)/p^m] \quad (5)$$

where $K(T)$ is the cooling function of the process and m is the Ozawa exponent that depended on the crystal growth and nucleation mechanism. The Ozawa equation can be rearranged into double-log form:

$$\log[-\ln(1 - X_t)] = \log K(T) - m \log p \quad (6)$$

Thus, plotting $\log[-\ln(1 - X_t)]$ against $\log p$ should yield a linear line with m as the slope and $\log K(T)$ as the intercept. The results of nonisothermal crystallization of PP and PP/starch composites analyzed with this method are shown in Figure 5. The non-linear lines indicated that m was not constant with increasing temperature during crystallization. It was impossible to estimate the cooling function $K(T)$ from the curvature lines, which implied that the Ozawa equation was inadequate in describing the nonisothermal crystallization kinetic of PP and PP/

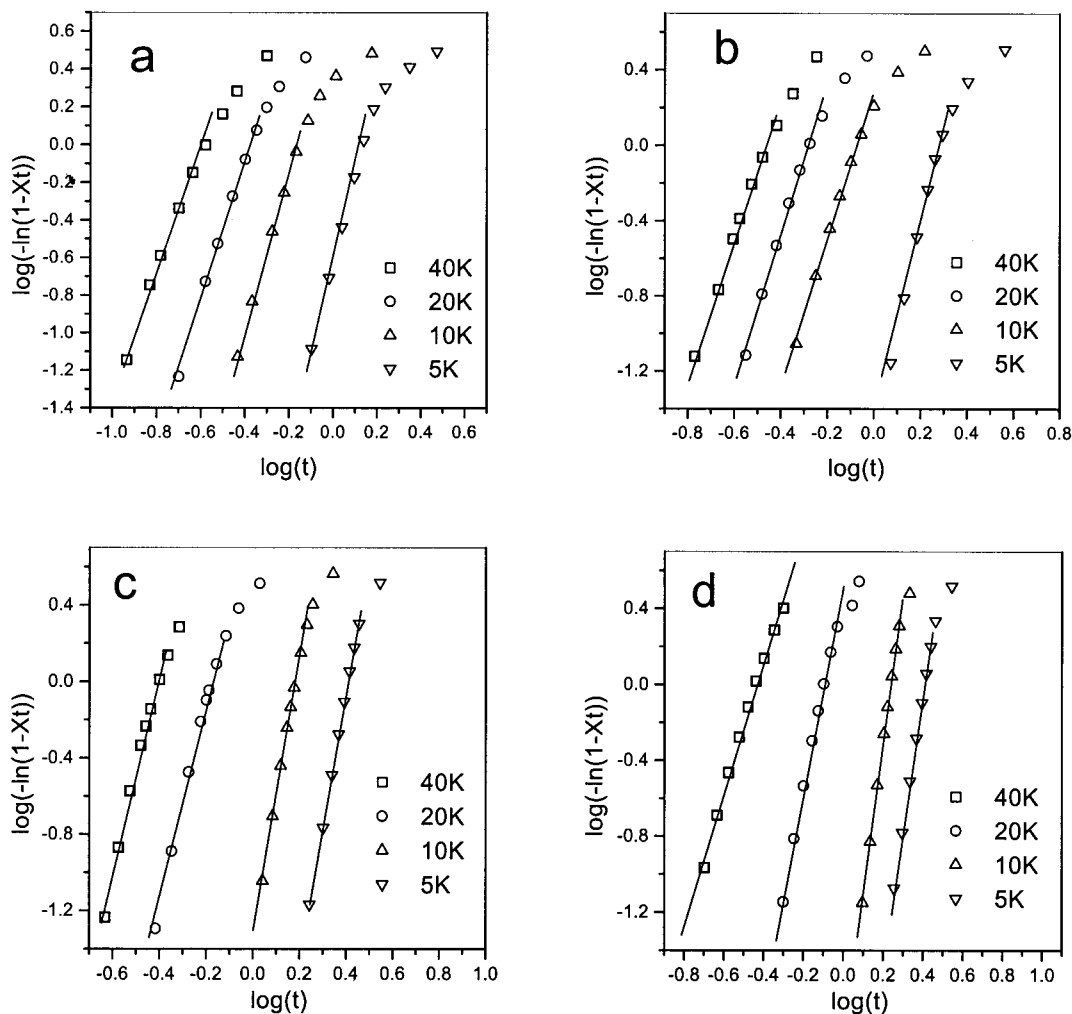


Figure 4 Plots of $\log[-\ln(1 - X_t)]$ versus $\log t$ for nonisothermal crystallization at different cooling rates of PP composites for (a) neat PP, (b) PP/amaranth starch, (c) PP/rice starch, and (d) PP/corn starch.

starch composites, possibly from the quasi-isothermal nature of the Ozawa treatment. The values of relative degree of crystallinity chosen at a given temperature included the values from the earliest stage of crystallization at a high cooling rate and values from the end stage at a low cooling rate. Therefore the nonisothermal crystallization kinetics should be different at different crystallization stages or different cooling rates.

Liu et al.²⁰ developed a new form of equation to accommodate the nonisothermal aspect of crystallization. For polymer processing of the nonisothermal crystallization, the nature of polymer was related to the degree of crystallinity X_t , cooling rate P , and crystallization temperature T . During the nonisothermal crystallization, the relationship between time and temperature of crystallization is given by

$$t = (T_0 - T)/p \tag{7}$$

where T is the crystallization temperature at crystallization time t and T_0 is the initial temperature at which crystallization begins ($t = 0$). For a given system at a given relative degree of crystallinity X_t and at crystallization time t , the following equation was obtained by combining eqs. (2) and (4).

$$\log k + n \log t = \log K(T) - m \log p \tag{8}$$

A new equation was obtained after rearrangement:

$$\log p = \log F(T) - a \log t \tag{9}$$

where $F(T) = [K(T)/k]^{1/m}$ refers to as the cooling rate at the unit crystallization time when the measured system reached a given degree of crystallinity, and $a = n/m$ is the ratio of the Avrami exponent n to the Ozawa exponent m . According to this equation, a straight line was produced by plotting $\log p$ against

TABLE II
Effect of Starch on the Crystallization Parameters of Polypropylene^a

| Sample | <i>P</i> (°C/min) | <i>n</i> | <i>K</i> | <i>t</i> _{1/2} (min) | <i>X</i> _c (%) |
|--------------------|----------------------|----------|------------------------|----------------------------------|------------------------------|
| PP | 40 | 3.2 | 7.4 × 10 | 0.23 | 56 |
| | 20 | 3.7 | 2.5 × 10 | 0.38 | 56 |
| | 10 | 4.0 | 4.1 | 0.63 | 58 |
| | 5 | 4.5 | 2.4 × 10 ⁻¹ | 1.26 | 59 |
| PP-amaranth starch | 40 | 3.7 | 5.5 × 10 | 0.31 | 56 |
| | 20 | 4.1 | 1.5 × 10 | 0.47 | 58 |
| | 10 | 4.0 | 2.0 | 0.76 | 58 |
| PP-rice starch | 40 | 4.4 | 5.7 × 10 | 0.36 | 53 |
| | 20 | 5.4 | 9.1 | 0.61 | 55 |
| | 10 | 7.3 | 4.6 × 10 ⁻² | 1.44 | 55 |
| PP-corn starch | 40 | 3.7 | 4.1 × 10 | 0.32 | 53 |
| | 20 | 5.5 | 3.6 | 0.74 | 55 |
| | 10 | 7.6 | 2.0 × 10 ⁻² | 1.64 | 55 |
| | 5 | 7.0 | 1.0 × 10 ⁻³ | 2.43 | 56 |

^a *P*, cooling rate during nonisothermal crystallization; *n* and *K*, Avrami index and crystallization rate constant in Avrami equation, respectively; *t*_{1/2}, half-time for crystallization; *X*_c, absolute degree of crystallization.

log *t* (Fig. 6). Values of *F(T)* and *a* were calculated from the intercept and slope of the lines, respectively, and are listed in Table III. *F(T)* increased as the relative degree of crystallinity increased, but the values of *a* were almost constant for a given system. With increasing starch granular size, both *F(T)* and *a* increased at a given relative degree of crystallinity.

Activation energy of nonisothermal crystallization

The method to evaluate activation energy under various cooling rates was proposed by Kissinger²¹:

$$\frac{d[\ln(p/T_p^2)]}{d(1/T_p)} = -\frac{\Delta E}{R} \tag{10}$$

where *R* is the universal gas constant. When plotting ln(*p/T_p²*) against 1/*T_p*, the activation energies of nonisothermal melt crystallization were determined and are summarized in Figure 7 and Table

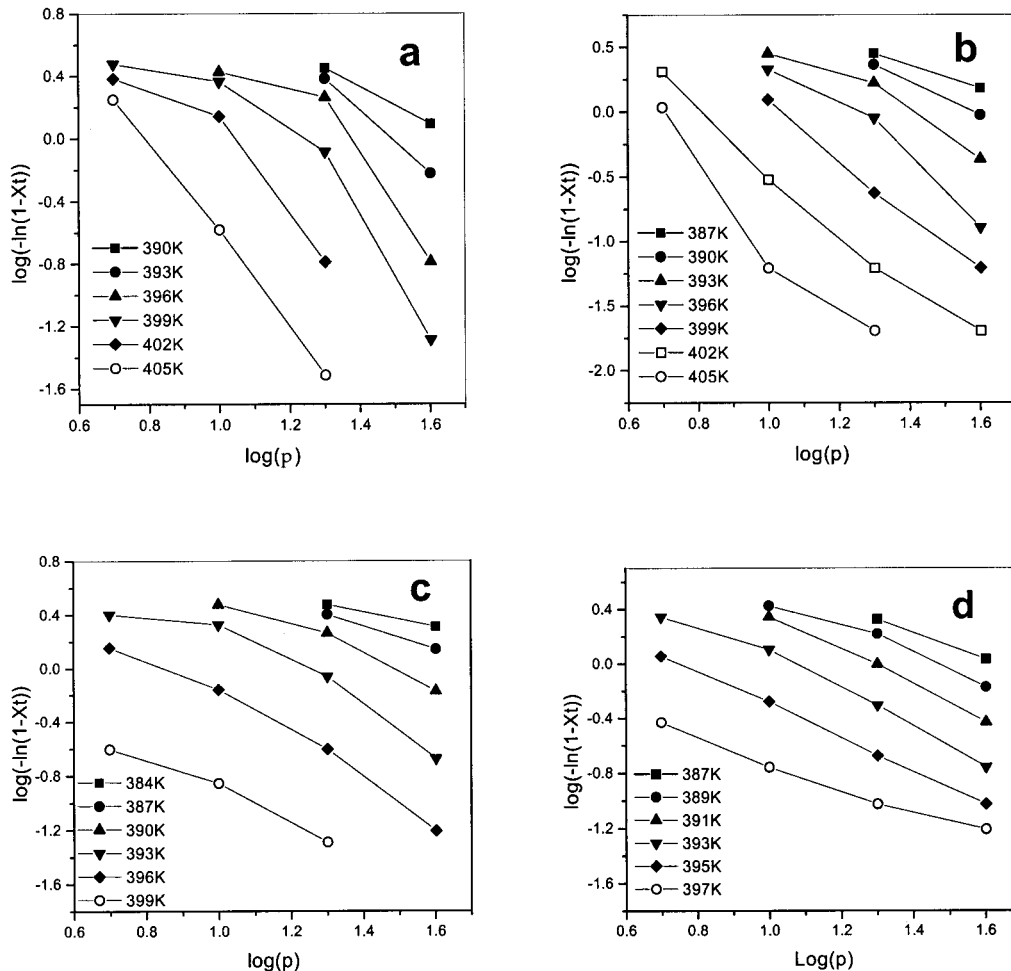


Figure 5 Ozawa plots of $\log[-\ln(1 - X_t)]$ versus $\log p$ for nonisothermal crystallization at different cooling rates of PP composites for (a) neat PP, (b) PP/amaranth starch, (c) PP/rice starch, and (d) PP/corn starch.

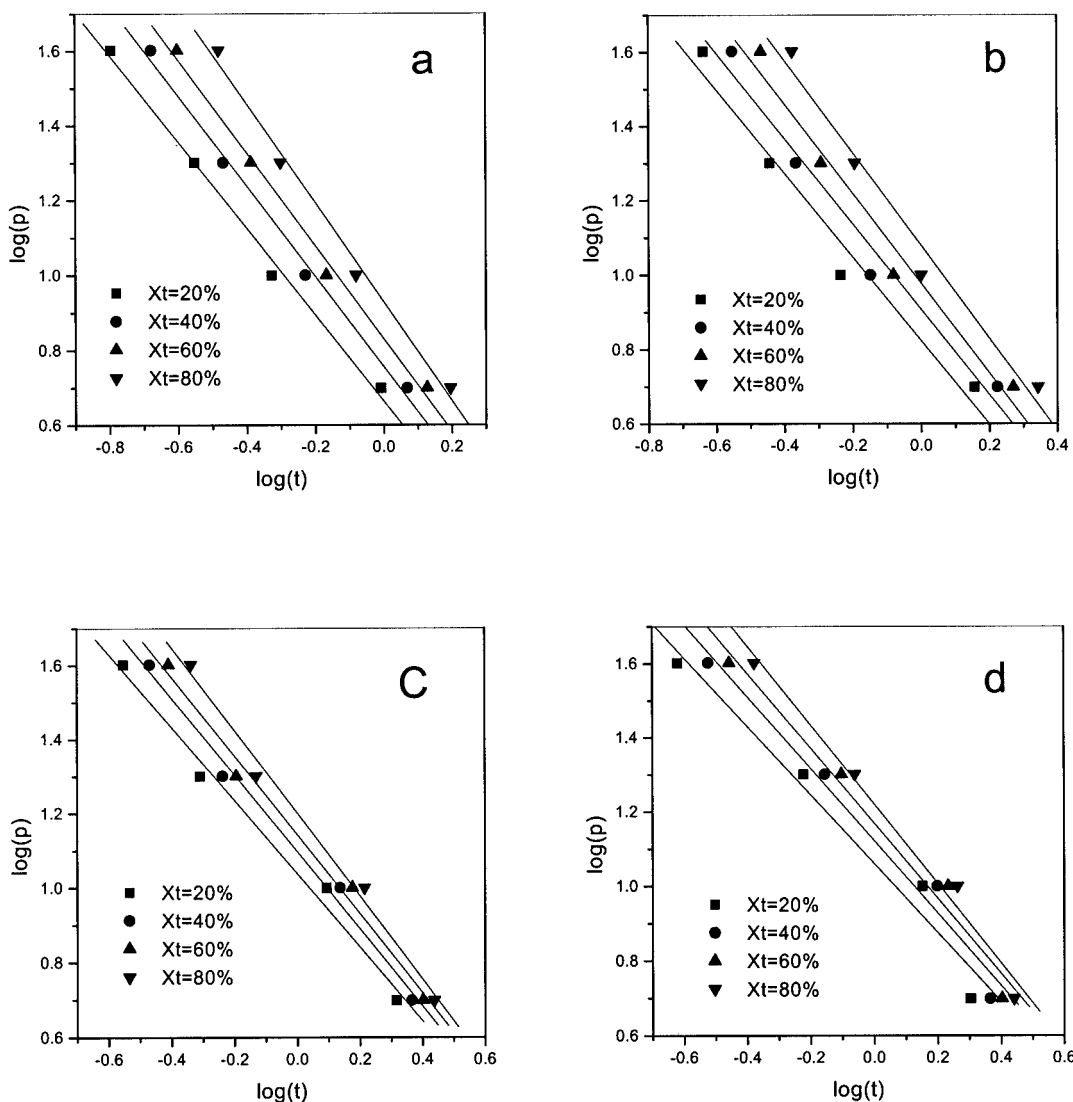


Figure 6 Plots of $\log p$ versus $\log t$ for nonisothermal crystallization at different cooling rates of PP composites for (a) neat PP, (b) PP/amaranth starch, (c) PP/rice starch, and (d) PP/corn starch.

III. The data showed that the crystallization activation of PP was lower than that of PP/starch composites and the crystallization activation of PP/starch composites increased with increasing starch granule size. It was possible that the presence of starch hindered molecular segments of PP transportation to the crystallization surface during cooling because of the interfacial tension of immiscible PP/starch blend. Additionally, the surface of starch is hydrophilic and mostly amorphous instead of crystalline. Therefore, hydrophobic PP molecular segment could not reach the surface of starch and crystallize. These two reasons led to an increase in the activation energy of nonisothermal crystallization of PP/starch composites compared with that of pure PP.

The difference in activation energy of different PP/starch composites reflected their difference in starch granule size. The PP/amaranth starch composites might have the smallest, whereas PP/corn starch composites might have the largest, interfacial tension. As the starch granule size increased, the interfacial tension increased accordingly, which impeded nucleus movement and transportation and resulted in a reduced crystallization rate of PP/starch composites. The activation energy results agreed with the morphology results of these composites.

CONCLUSIONS

The dispersion of starch in PP was homogeneous, although starch and PP were not compatible. Starch

reduced the crystallization temperature and rate of PP at a given cooling rate under the condition of nonisothermal crystallization. The Ozawa equation was inadequate in describing the nonisothermal crystallization behavior of starch-filled PP because of the quasi-isothermal character of the Ozawa treatment. The Avrami method was used to analyze the crystallization process and calculate the crystal parameters. A new method combining the Avrami and Ozawa equations was appropriate to explain the nonisothermal crystallization of starch-filled PP. The decrease in crystallization rate and increase in activation energy significantly correlated with increasing starch granule size.

The authors thank Devon Cameron for preparing amaranth starch. This work was financially supported by the Agricultural Experiment Station at the University of Arkansas and the Arkansas Rice Research and Promotion Board.

TABLE III
Effects of Starch on the Crystallization Parameters of Polypropylene^a

| Sample | X_t | $F(t)$ | a | ΔE (kJ/mol) |
|--------------------|-------|--------|------|---------------------|
| PP | 20 | 4.6 | 1.13 | 239.2 |
| | 40 | 5.6 | 1.20 | |
| | 60 | 6.8 | 1.24 | |
| | 80 | 8.5 | 1.32 | |
| PP-amaranth starch | 20 | 6.6 | 1.12 | 269.7 |
| | 40 | 8.1 | 1.15 | |
| | 60 | 9.6 | 1.20 | |
| | 80 | 12.0 | 1.24 | |
| PP-rice starch | 20 | 10.7 | 1.00 | 440.3 |
| | 40 | 12.6 | 1.04 | |
| | 60 | 13.8 | 1.06 | |
| | 80 | 15.9 | 1.11 | |
| PP-corn starch | 20 | 11.5 | 0.92 | 449.9 |
| | 40 | 13.2 | 0.97 | |
| | 60 | 14.8 | 1.01 | |
| | 80 | 16.6 | 1.06 | |

^a X_t , relative degree of crystallinity; $F(t)$, cooling rate at the unit crystallization time when the measured system reached a given degree of crystallinity; a , ratio of the Avrami exponent n to the Ozawa exponent m ; ΔE , activation energy during nonisothermal crystallization.

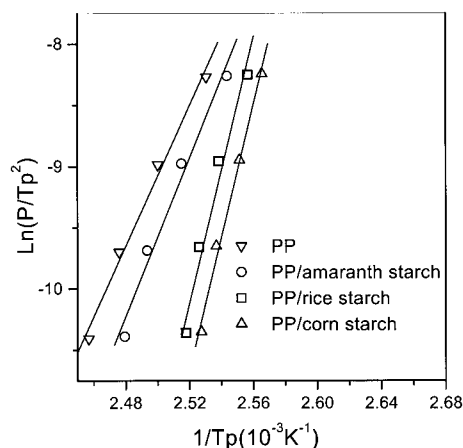


Figure 7 Kissinger plots for evaluating nonisothermal crystallization activation energies of PP composites for (a) neat PP, (b) PP/amaranth starch, (c) PP/rice starch, and (d) PP/corn starch.

References

- Busigin, C.; Lahtinen, R.; Thomas, G.; Woodhams, R. T. *Polym Eng Sci* 1984, 24, 169.
- Liu, J.; Wei, X.; Guo, Q. *J Appl Polym Sci* 1990, 41, 2829.
- Maiti, S. N.; Mahapatro, P. K. *J Appl Polym Sci* 1991, 42, 3101.
- Liu, J.; Tang, G.; Qu, G.; Zhou, H.; Guo, Q. *J Appl Polym Sci* 1993, 47, 2111.
- Tjong, S. C.; Li, R. K. Y.; Cheung, T. *Polym Eng Sci* 1997, 37, 166.
- Chen, X.; Guo, Q.; Mi, Y. *J Appl Polym Sci* 1998, 69, 189.
- Mayer, J. M.; Kaplan, D. L. *Trends Polym Sci* 1994, 2, 227.
- Hamdan, S.; Hashim, D. M. A.; Ahmad, M.; Embong, S. *J Polym Res* 2000, 7, 237.
- Weil, R. C. U.S. Pat. 5,026,745, 1991.
- Li, B.; Sun, C.; Zhang, T. *Poly Mater Sci Eng* 2000, 16, 146 (in Chinese).
- Bagheri, R. *Polym Int* 1999, 48, 1257.
- Yang, C.-C.; Lai, H.-M.; Lii, C.-Y. *Food Science* 1984, 11, 158.
- Paul, D. R.; Newman, S. *Polymer Blends*, Vol. 1; Academic Press: New York, 1978.
- Shariatpanahi, H.; Nazokdast, H.; Dabir, B.; Sadaghiani, K.; Hemmati, M. *J Appl Polym Sci* 2002, 86, 3148.
- Bartczak, Z.; Galeski, A.; Krasnikova, N. P. *Polymer* 1987, 28, 1627.
- Long, Y.; Shanks, R. A.; Stachurski, Z. H. *Prog Polym Sci* 1995, 20, 651.
- Avrami, M. *J Chem Phys* 1939, 7, 1103.
- Avrami, M. *J Chem Phys* 1940, 8, 212.
- Ozawa, T. *Polymer* 1971, 12, 150.
- Liu, T. X.; Mo, Z. S.; Wang, S. E.; Zhang, H. F. *Polym Eng Sci* 1997, 37, 568.
- Kissinger, H. E. *J Res Natl Bur Stand (US)* 1956, 57, 217.